SUBMESOSCALE EDDY TRAPPING SUPPORTS PLANKTONIC ACTIVITY BEYOND THE COASTAL UPWELLING ZONE

ÉLISE BEAUDIN[a], DANTE A. CAPONE[b], SARAH E. LANG[c], MELISSA M. OMAND[c], EMANUELE DI LORENZO[a], MOIRA DÉCIMA[b], AND MARA A. FREILICH[a,d]

Abstract. Eastern boundary current systems are among the most productive marine ecosystems, sustained by coastal upwelling that brings cold, nutrient-rich waters to the surface. While this process fuels high primary productivity nearshore, the offshore region remains nutrient-depleted. Mesoscale eddies (∼100 km) are known pathways that transport nutrients into the open ocean, yet recent high-resolution satellite imagery reveals that smaller submesoscale eddies (∼10 km) may also contain elevated chlorophyll at their cores. Here, using multi-platform observations from in situ and airborne measurements, we show that submesoscale eddies support primary production offshore. We extensively surveyed a submesoscale eddy about 300 km off the US west coast that transported and sustained elevated chlorophyll concentrations over several weeks, demonstrating strong biophysical coupling at these scales. Moreover, we find that the export flux of organic material from submesoscale eddies is comparable to that of mesoscale eddies, indicating that submesoscale eddies are integral to eddy-driven lateral advection across gyre margins and into the depleted subtropical gyres. This study provides observational evidence that submesoscale eddies act as localized ecological niches that shape and sustain productivity beyond the coastal upwelling zone, and should therefore be considered in assessments of the ocean's carbon transport and cycling.

Eastern boundary currents support some of the most productive marine ecosystems globally. Strong coastal winds drive upwelling, supplying the coast with nutrient-rich waters that fuel intense marine productivity [1]. In contrast, reduced nutrient availability offshore in the subtropical gyre leads to a strong cross-shore gradient in productivity and biomass between the continental margin and the gyre interior [2, 3]. Turbulent oceanic features such as eddies and filaments can act as pathways for advecting coastal waters into the oligotrophic open ocean, generating spatial heterogeneity in productivity and fluxes that translate into complex patterns of surface chlorophyll concentration [4, 5].

In the California Current System (CCS), mesoscale eddies and upwelling filaments are traditionally regarded as the primary drivers for offshore nutrient fluxes due to their large areas (∼100 km), prevalence, and longevity [6, 7, 8, 9]. Beyond their role in water mass trapping and transport [10], eddies can have myriad effects on marine ecosystems including modulating vertical nutrient supply, generating biological niches, and altering predator-prey interactions [2, 11, 12, 13, 5]. Submesoscale eddies, which are much smaller (0.1-1 km) than mesoscale eddies and evolve on timescales of days, are increasingly recognized as a key contributors to the physical and biological dynamics of coastal regions, yet remain challenging to observe [14, 15]. These shorter-lived, smaller features arise from instabilities in the stratified flow field [16, 17, 18], and are associated with small-scale vertical motions that strongly influence surface phytoplankton variability [19, 20, 21]. At these spatial and temporal scales, biological processes such as phytoplankton growth, grazing, and natural mortality can respond to physical forcing in ways that further shape surface chlorophyll distributions [22, 23, 24].

Productivity at the submesoscale is shaped by interactions between biological and physical processes; yet, the relative contributions of these processes, as well as coherent lateral transport, remain poorly quantified observationally at the submesoscale. Here, we use novel high-resolution observations of surface currents and biological productivity within a submesoscale eddy to simultaneously quantify the contributions of physical and biological processes to submesoscale surface phytoplankton variability. These observations overcome the limitations of previous observations of surface currents to allow quantification of vertical velocity at the submesoscale. We combine high-resolution observations of ocean physics with co-located measurements of phytoplankton growth and microzooplankton grazing rates conducted in a water mass following frame. These combined observations reveal the complex interplay between physics and biology that occurs within submesoscale eddies and demonstrates that biological processes and coherent trapping can act as the main drivers controlling surface phytoplankton hotspots, rather than vertical nutrient flux. We show that submesoscale eddies, through trapping of surface waters, can serve as regulators for coastal regions' influence on surface phytoplankton biomass and carbon fluxes in an offshore eastern boundary current region.

Methods

This study was conducted using observations from the S-MODE IOP-2, which took place between April 9 and May 2, 2023, on board the RV *Sally Ride*, at approximately 300 km offshore San Francisco (Fig.1a). We integrate co-located physical and biological measurements profiled and sampled from the ship and other airborne instruments at the surface and subsurface. A full description of the expedition can be found at [25].

Chlorophyll Rates of Change Estimation We derive the rate of change of surface chlorophyll from a Lagrangian perspective for 136 microstar (1 m drogue) and CARTHE (60 cm drogue) drifters released during the campaign (`https://doi.org/10.5067/SMODE-DRIFT`). When a drifter is found within a 1 km radius of the ship, we assign chlorophyll, temperature, and salinity values measured from the ship (`https://doi.org/10.5067/SMODE-RVECT3`) (Fig.2). Chlorophyll measurements from the ship were considered co-located with the drifter when the ship was within 1 km of its position. The 1-km value is based on the typical spatial variability of chlorophyll and the need to retain a sufficient number of data points for the analysis.

Since drifters are buoyant and stay near the surface, we can detect subduction of a water parcel by observing abrupt changes in physical properties (e.g., temperature, salinity) and only keep the time series for water parcels where those properties remain relatively stable. Chlorophyll rates of change within moving water parcels are then estimated using:

$$\frac{\mathrm{D}_h P(t)}{\mathrm{D}t} \approx P(t) \cdot \left(\frac{\log\left[P(t)/P(t-\Delta t)\right]}{\Delta t} \right) \tag{1}$$

where the subscript h indicates that we only consider the horizontal Lagrangian derivative:

$$\frac{\mathrm{D}_h}{\mathrm{D}t} = \frac{\partial}{\partial t} + u\frac{\partial}{\partial x} + v\frac{\partial}{\partial y} \tag{2}$$

This approach helps us isolate the impact of local processes by removing the effects of lateral advection, allowing us to quantify intrinsic changes in chlorophyll concentration as water parcels move horizontally with the flow.

The standard error is derived from the expected variability in chlorophyll concentration as a function of spatial separation. Specifically, we calculated the standard deviation of chlorophyll

differences between points along the ship track at increasing separation distances. This relationship was then used to assign uncertainty based on the distance between the ship measurement and the drifter location it was assigned to.

Surface Kinematics and Okubo-Weiss Parameter We use kinematic properties of the flow to identify the submesoscale features. We define the relative vorticity (ζ) and divergence (δ) of

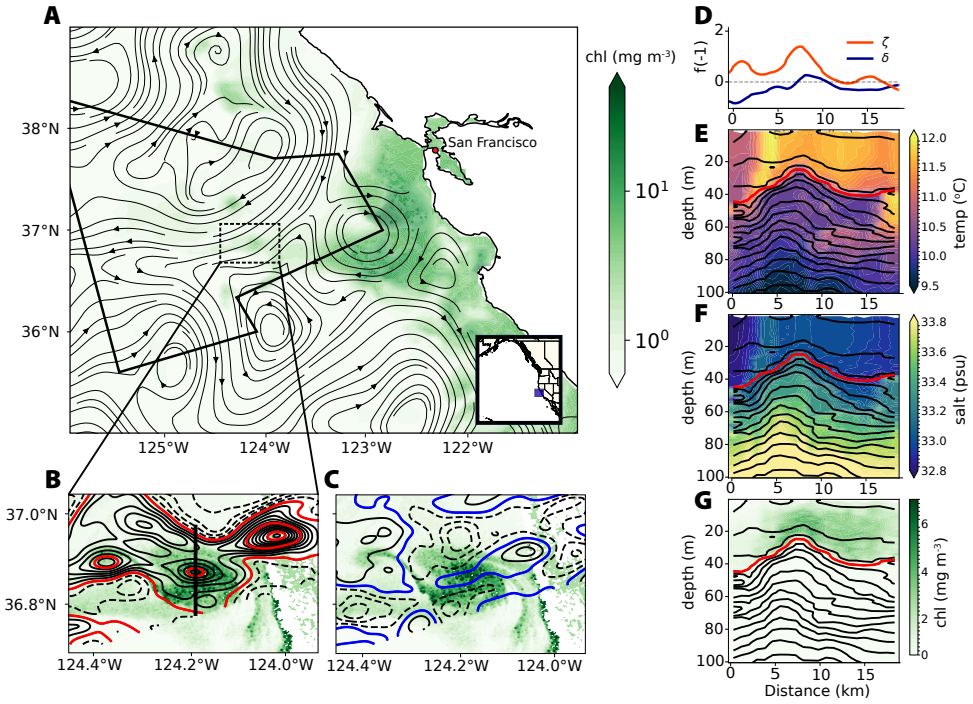

FIGURE 1. Satellite, airborne, and in situ observations of a submesoscale eddy. (a) Multi-sensor (Sentinel-3 OLCI, MODIS-Aqua, VIIRS) imagery at 4-km resolution of chlorophyll concentration in the California Current System on April 22, 2023, with the mesoscale surface currents from AVISO (streamlines). The S-MODE operation area is outlined within the black polygon. The box indicates the region shown in panels (b) and (c), which display Sentinel-3A OLCI imagery at 300-m resolution of surface chlorophyll concentration with surface vorticity and surface divergence (contours), respectively, with colored contours at -1, 0, and 1. The black line in (b) marks the ship's transect sampling location for panels (e-g). (d) Values of vorticity and divergence across the black line. Vertical sections of (e) absolute salinity, (f) conservative temperature, and (g) chlorophyll concentration, with the mixed-layer depth (red solid line).

the flow as:

$$\begin{aligned} \zeta &= v_x - u_y \\ \delta &= u_x + v_y \end{aligned} \tag{3}$$

where u and v are the 1 m-depth full flow velocities estimated from the Ka-band Doppler Scatterometer (DopplerScatt), which is an airborne instrument that provides simultaneous measurements of ocean surface currents and vector winds at 200 m spatial resolution over a 24-km swath using radar backscatter. (`https://doi.org/10.5067/SMODE-DSCT2-V2`). Unless mentioned, all the kinematic properties of the flow are normalized by the Coriolis parameter f. We assume that these measurements are representative of the drifters' depth, allowing us to integrate them with the drifters' Lagrangian positions.

Following Tarry et al. (2022), we obtain the vertical velocity (w) at depth by integrating the continuity equation ($u_x + v_y + w_z = 0$) from a reference level h_0 where w is known:

$$w(z = h) - w(z = h_0) = \int_{h_0}^{h} (u_x + v_y) dz \tag{4}$$

Assuming that the surface vertical velocity (w at $h = 0$) is negligible and that the estimated divergence is constant within the top layer, the vertical velocity at depth h is:

$$w(h) = -h \cdot \delta \tag{5}$$

From this expression, we infer that a positive divergence indicates convergence of the surface waters leading to downwelling, and vice versa.

The Okubo-Weiss (OW) parameter was computed from the horizontal velocity field as:

$$\mathrm{OW} = s_n^2 + s_s^2 - \zeta^2 \tag{6}$$

where the normal strain (s_n), shear strain (s_s) are defined as:

$$s_n = u_x - v_y \tag{7}$$

$$s_s = v_x + u_y \tag{8}$$

Negative values of OW indicate rotation-dominated, coherent eddy cores, while positive values indicate strain-dominated, filamented regions.

Growth and Grazing Rate Experiments We computed rates of phytoplankton community growth and microzooplankton grazing on phytoplankton using chlorophyll-α analyses of dilution incubation experiments [26]. 24-hour experiments were initiated between 1AM and 8AM in 3 incubators with light levels corresponding to approximately 1%, 10%, and 70% of surface PAR. Here we utilize only experiments conducted in the 1% light level or surface water (5 m-depth). We used dilution fractions of 10%, 33%, and 100% whole seawater. Seawater was filtered directly from the Niskin bottles with a peristaltic pump, acid-washed silicone tubing, and a 0.1-μm Acropak filter that had previously been acid washed. Incubation bottles were first filled with the volume of filtered water and then gently topped off with unfiltered water from the Niskin bottles to avoid physical damage to fragile protists.

Apparent phytoplankton growth rates were measured across dilution fractions and fit to the linear model:

$$\mu(D) = m - g(1 - D),$$

where $\mu(D)$ is the observed net growth rate at dilution fraction D, m is the intrinsic phytoplankton growth rate (intercept), and g is the microzooplankton grazing mortality rate (negative slope).

When appropriate, we included either a nutrient amended experiment or added nutrients to the full grazing profile. We used recommendations by [27] to select concentrations of 44 mM $NaNO_3$ and 36.6 mM $NaPO_4$ to add to selected bottles. Initial chlorophyll a samples were taken by filtering 565-570 mL of water from the Niskin onto a 25 mm diameter Whatman GFF and final measurements were taken using 290 mL of water incubation bottles. The filters were placed in 6 mL test tubes of 90% acetone and refrigerated at -20^{o}C in the dark for 24-48 hours before the measurement was read using a Turner 10-AU fluorometer. We calculated growth and grazing rates and associated standard errors of the slope and intercept as the linear regression between dilution fraction and apparent growth rate, as detailed in [26].

Experiments that violated assumptions of the dilution experiments laid out in [26] and displayed a positive slope (increasing apparent growth rate with increasing fraction whole seawater) were addressed in two ways. First, if the standard error of experiments with a positive grazing rate contained zero in the lower bound of the 95% CI, that rate was set to zero. If the standard error did not contain zero in the lower bound of the 95% CI, that rate was set to NA and discarded.

AC-S: Spectral Absorption and Attenuation Measurements Underway chlorophyll-α concentrations at 4-m depth were estimated using the absorption line height at 657 nm, measured by an AC-S Spectral Absorption and Attenuation Sensor [28, 29]. These measurements were used to validate satellite estimates of surface chlorophyll and to identify surface chlorophyll maxima in cases where the underway fluorometer was affected by non-photochemical quenching.

Budget Analysis The budget analysis is conducted within a Lagrangian framework, which allows us to ignore horizontal advective contributions and focus solely on the local changes occurring within a water parcel. We consider two main biological processes: net phytoplankton growth and grazing by zooplankton, and one physical process: vertical advection. The latter contributes to the variability by either bringing up or drawing down planktonic matter to the surface. The total rate of change in surface phytoplankton biomass within a water parcel can be expressed as:

$$\frac{\mathrm{D}_h P}{\mathrm{D}t} = G - \Gamma - w\frac{\partial P}{\partial z} + residual \tag{9}$$

where h indicates the horizontal derivative, G is the net growth rate of phytoplankton (including growth, respiration, and mortality), Γ is the grazing rate of phytoplankton by zooplankton, and $w\frac{\partial P}{\partial z}$ is the vertical advection of phytoplankton. The residuals include processes that were neglected or not measured, such as internal mixing, non-linear response of phytoplankton to nutrient inputs, diffusion of the water parcel to its surroundings, and lateral entrainment of surrounding waters to the water parcel. We estimate w, the vertical velocity, from surface divergence (δ). $\frac{\partial P}{\partial z}$ is estimated from the difference in chlorophyll concentration between 4 m-depth AC-S measurements and 18 m-depth ship measurements.

Submesoscale Eddy Count To estimate the number of submesoscale eddies in the offshore region, we used satellite chlorophyll data from two different spatial resolutions: a 300-m high-resolution dataset and a coarser 4-km resolution dataset, both from the Copernicus Sentinel-3 Ocean and Land Colour Instrument (OLCI). We counted by hand the number of eddies smaller than 100 km that had high concentration of chlorophyll and had crossed 124°W between 36°N

and 39°N. Despite the difference in resolution, both datasets yielded similar counts of submesoscale eddies over the past years, with annual numbers ranging between 10 and 30.

Export Flux Calculation To estimate the lateral export of particulate organic carbon (POC) associated with submesoscale eddies, we computed the flux as the product of eddy velocity (U), POC concentration (C), and the fractional coverage of submesoscale eddies (P) across a zonal section from 36°N to 39°N. The average surface velocity was derived from DopplerScatt trajectories, while near-surface POC concentration was inferred from shipboard measurements. Eddy fractional coverage, P, was estimated by counting submesoscale eddies observed daily in satellite imagery over two years and assuming a representative eddy diameter of 5 km. The final export flux per unit area was computed as:

$$Flux = U \cdot C \cdot P \tag{10}$$

Flux uncertainty was estimated by propagating the standard deviations of each term under the assumption that they are independent from each other.

Results

Submesoscale eddies retain and transport coastal organic material Satellite observations of surface chlorophyll concentration in the CCS show a highly heterogeneous pattern (Fig.1a). As is typical, a strong cross-shore gradient in surface chlorophyll concentration is apparent from low spatial resolution (4 km) imagery, with elevated chlorophyll concentrations near the coast to near-zero offshore. While the chlorophyll pattern aligns in some regions with mesoscale features, the offshore oligotrophic region exhibits a few productive hotspots, with characteristic sizes of ∼10 km and chlorophyll concentrations of about 5-10 mg m^{-3} that do not align with mesoscale velocity streamlines, suggesting an influence of submesoscale processes.

By contrast, combining high-resolution satellite imagery of surface chlorophyll with airborne velocity observations reveals the nature of these submesoscale features (Fig. 1b). The airborne velocity estimates are obtained from DopplerScatt, which provides the total surface ocean velocity vector over 24 km swaths at 200 m spatial resolution. This is in contrast to previous studies that have relied on geostrophic velocities or shipboard observations. We first present an intensive study of a single submesoscale eddy over its temporal evolution before quantifying the contribution of these types of features, which are prevalent in the California Current System, to carbon fluxes. The surface relative vorticity, a measure of vortical motion computed through velocity gradients, exhibits a coherent pattern that is closely aligned with surface chlorophyll (Fig. 1d), with relative vorticity reaching values of $1.5f$, values typical of submesoscale dynamics. We find much less correspondence between chlorophyll and the divergence field. The divergence field, indicative of upward and downward movements of surface water masses, has a more temporally variable spatial structure (SI Appendix, Fig. S2). At times, it has a dipole shape with weak positive divergence values of $0.2f$ near the core, suggesting a weak upwelling. Strong negative values at the northern and southern edges of the eddy, -0.9f and -0.5f, respectively, suggest downwelling at the edges. However, the core also intermittently exhibits downwelling. These observations demonstrate the rapidly evolving nature of submesoscale dynamics, which can complicate assessment of their impact on ocean productivity from single snapshots alone.

While some evidence points to increased productivity in the eddy core due to vertical transport (positive divergence, which corresponds to upward nutrient and carbon flux), the physical retention of coastal biological material appears to be the primary mechanism that contributes to the offshore biomass hotspot within the eddy. On average over the sampling period, the surface divergence was negative within the eddy, suggesting only episodic upwelling. During the

observational period, the eddy was interacting with a filament at its northern edge, contributing to deformation and rapid dynamical changes that may affect productivity. In addition to the coherent vorticity pattern, ship-based observations of temperature and salinity show that water trapped within the eddy core near 36.88°N is colder and saltier than surrounding waters (Figs. 1e,f; SI Appendix, Fig. S1), further suggesting trapping of a distinct water mass. This trapping of surface waters aligns with elevated chlorophyll concentrations, suggesting that coastal planktonic material is retained in the eddy core (Fig. 1g). Although the peak chlorophyll fluorescence is found within the mixed-layer, discrete samples and AC-S measurements confirm that the maximum chlorophyll concentration is at the surface.

Based on surface and transect measurements of particulate organic carbon (POC), and assuming constant concentrations from the surface to 25 m depth, we estimate a POC inventory of approximately 2.87 Gg (±1.0 Gg) within the coherent submesoscale eddy (see Methods). This mass is transported offshore at an average observed velocity of 0.1 (± 0.05) ms^{-1} during the observation period. Assuming the eddy began with typical coastal surface chlorophyll concentrations of around 10-20 mg m^{-3}, the observed offshore concentration of ∼5 mg m^{-3} suggests an e-folding decay timescale of 2-3 weeks. This timescale is longer than previously reported loss rates of order days for the CCS [30, 31], which may indicate that slower biological processes contribute to chlorophyll removal within submesoscale eddies. Alternatively, this could suggest that underlying physical and biological mechanisms acted to maintain elevated concentrations during transit, possibly with eddy-induced growth. Lagrangian rates of change of surface chlorophyll in the offshore region across all drifter observations during the field campaign — not limited to the coherent eddy — ranged from -6 to 5 mg m^{-3} day^{-1} (Fig. 2c).

These combined biophysical, submesoscale resolving observations demonstrate that submesoscale hotspots of chlorophyll, defined as ellipses that are $\mathcal{O}(10\ km)$ in radius are coherent submesoscale eddies that propagate westward. Examining the full dataset, our observations suggest that submesoscale coherent eddies constitute a significant lateral carbon flux in this eastern boundary current region. Based on an analysis of Sentinel-3A OLCI satellite chlorophyll, we observe between 10-30 submesoscale eddies that cross 124°W (about 300 km from the coast), per year, between 2022 and 2025 (SI Appendix, Table S1). We are unable to systematically track the eddies due to cloud cover, but we estimate that between 36°N and 39°N, submesoscale eddies laterally transport POC at an average rate of -0.0434 ± 0.0237 mmol C m^{-2} s^{-1}, with the negative sign indicating westward cross-shore transport. The relatively large uncertainty mostly reflects natural variability in the eddy velocity and the number of active eddies at any given time. Our estimates of POC transport are conservative, as they rely on eddy detection using daily snapshots of satellite-derived chlorophyll, which are frequently affected by cloud cover.

Biophysical coupling drives surface phytoplankton abundance variability The observed persistence of elevated concentrations at the eddy surface and subsurface after several days of propagation suggests that there are underlying mechanisms responsible for this sustained productivity or that, alternatively, the chlorophyll loss processes are relatively slow, resulting in efficient trapping and transport coastal organic material in the oligotrophic offshore region. This highlights the important contribution of this coherent eddy for offshore carbon flux.

Coherent submesoscale trapping is an important factor in the offshore evolution of the high biomass feature. Coherent eddies can undergo minor deformation and stretching throughout their lifespan allowing them to retain most of their biomass within their core [32, 33]. In contrast, eddies that lose coherence leak their contents and gradually lose biomass to the surrounding waters. Surface chlorophyll concentration (Fig. 3b) is highest within the core

($\sim$5 mg m^{-3}) and declines to $\sim$1 mg m^{-3} farther away, signifying that the eddy traps the high-chlorophyll waters within its core despite leakage to the surrounding water. A composite of the submesoscale eddy's kinematic properties (Fig. 3a), constructed from five aerial snapshots of surface currents (SI Appendix, Fig. S2), reveals a coherent structure characterized by a strong cyclonic core and weak surface convergence. The zero contour of the Okubo-Weiss parameter was used to delineate the eddy's outer edge [34, 35, 36]. The consistency of vorticity and velocity fields across multiple days suggests that the eddy maintains a stable core, which, coupled with the observation of high chlorophyll even in the presence of downwelling, indicates a dynamically stable structure capable of trapping and transporting material over at least days to weeks. Indeed, the eddy trapped 5 drifters for 5 days. These drifters are used to estimate Lagrangian rates of change of chlorophyll within the eddy.

The eddy appears to act as an incubator for phytoplankton growth. At night, when we expect no net biological growth, chlorophyll generally declines in the core. During the day, growth persists near the core despite downwelling. These results suggest that daytime biological productivity within the eddy is key to sustaining chlorophyll. However, weak downwelling near the core likely contributes to vertical export to greater depths, which can deplete surface waters of organic material.

Although the eddy core remains coherent during the observational period, the feature interacts dynamically with its surroundings, producing complex temperature, salinity, and chlorophyll patterns at its edges (Fig. 1e,f; see the warmer, fresher intrusion in the mixed layer at the northern edge). Dynamics at the edge are substantially different from the core. At the edge,

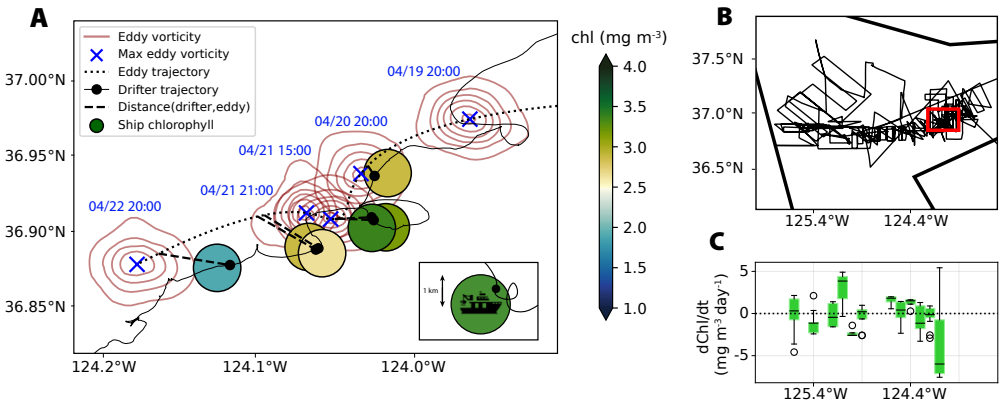

FIGURE 2. Tracking chlorophyll variability within water parcels. (a) Transition from a Eulerian to a Lagrangian framework, integrating drifter and ship observations. The drifter trajectory is shown as a black line. Chlorophyll values from the ship (green circles) were assigned to the drifter when the ship was within 1 km. The submesoscale eddy (grey circles) was mapped using Doppler-scatt, with its core position (blue crosses) interpolated over time (dotted line). Dashed lines represent the distance between the drifter with assigned chlorophyll values and the eddy core at corresponding times. (b) Full ship track as thin black line, with the area of interest indicated by the red box. (c) Chlorophyll rate of change across the green line in (b).

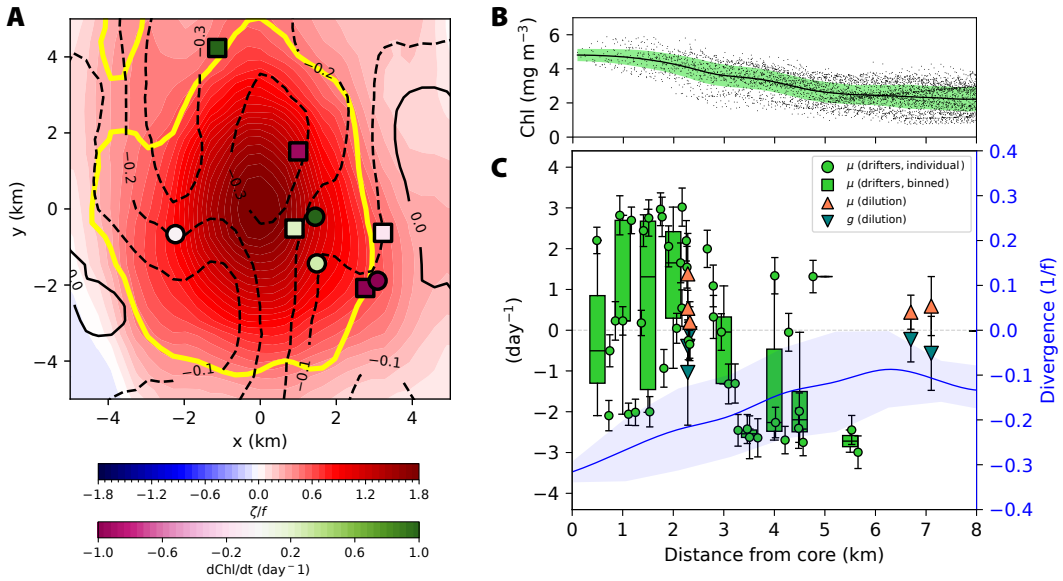

FIGURE 3. Composite analysis of the submesoscale eddy. Composited (a) surface vorticity (colors), divergence (black lines), and zero-crossing of the Okubo-Weiss parameter (yellow line), with chlorophyll rates of change averaged over 12-hour periods for daytime (circles) and nighttime (squares), (b) radially-averaged ship-based chlorophyll concentration, and (c) specific chlorophyll rate from drifters, specific growth and grazing from dilution experiment, and radially-averaged divergence, against the distance from the eddy core.

there is a filamentous pattern of chlorophyll that varies day by day. Submesoscale dynamics including cyclostrophic effects and frontal strain may cause exchange with surrounding waters and shedding of high biomass filaments, demonstrating one mechanism by which submesoscale eddies impact their distribution. The rate of change of chlorophyll at the edge varies on diel and longer timescales, likely due to interactions with surrounding water in addition to diel variability. However, on average the chlorophyll decays at the edge. Observed rates of change of chlorophyll account just for change at the surface rather than fully Lagrangian trajectories. As a result, we interpret the changes at the edge as due to a combination of biological processes and downwelling of dense filaments that are shed off the cyclone.

The rates of change of surface chlorophyll with respect to the distance from the core shown on Fig. 3c suggest complex dynamics: within 2 km of the eddy center, chlorophyll rates of change vary widely (± 2 per day), while values beyond 2 km of the eddy center are mostly negative, reaching -3 per day. The negative divergence within the eddy, indicative of downward vertical motion, points to vertical advection as a driver for loss near the core. However, this mechanism alone cannot account for the observed gain in surface chlorophyll, implying that other mechanisms are also influencing surface productivity. We propose that non-linear biological responses to vertical motion within the eddy core account for the predominance of growth in this region.

Growth and grazing rates exhibit spatial variability that is comparable in magnitude to the observed chlorophyll rate of change, although their net contribution appears to be small (Fig. 3C). Within ∼1 km of the eddy core, net specific growth and grazing rates nearly cancel out, resulting in minimal net biomass change. At around 2 km from the core, net growth dominates, with values up to 1.4 per day, while grazing reaches a magnitude of -1.0 per day. Beyond 6 km, outside the eddy's sustained influence, growth and grazing rates remain large (0.4 and 0.6 per day), indicating persistent biological activity. While the rates may fluctuate across the five-day observation window, net growth seems to be generally more important than biological decay, suggesting that biological activity is an important factor contributing to reducing the rate of phytoplankton decay inside the eddy.

Quantifying the relative contributions of physical and biological processes We computed a chlorophyll budget to quantify the net and respective contributions of biological processes and physical transport to surface chlorophyll variability (Fig. 4a). Biological processes are represented as net growth minus grazing while physical transport is represented as vertical advection of particulate carbon ($w \cdot \partial P/\partial z$). We quantified the relative importance of each mechanism separately over time, with a 12-hour integrated periods, to distinguish between daytime and nighttime variability. The Lagrangian rate of change of chlorophyll exhibits strong variability, ranging from -1.2 to 1.6 per day with a median value of -0.3 per day, indicating overall decay. In the absence of strong biological growth, physical export becomes dominant in driving chlorophyll decay.

Vertical advective flux is always negative, with a minimum value of -1.2 per day, resulting in a loss of chlorophyll from the surface. This is due to the negative averaged surface divergence. Phytoplankton carbon increases towards the surface, resulting in a positive gradient and a negative (downward) flux. The decline of vertical advective flux over time is due to weakening

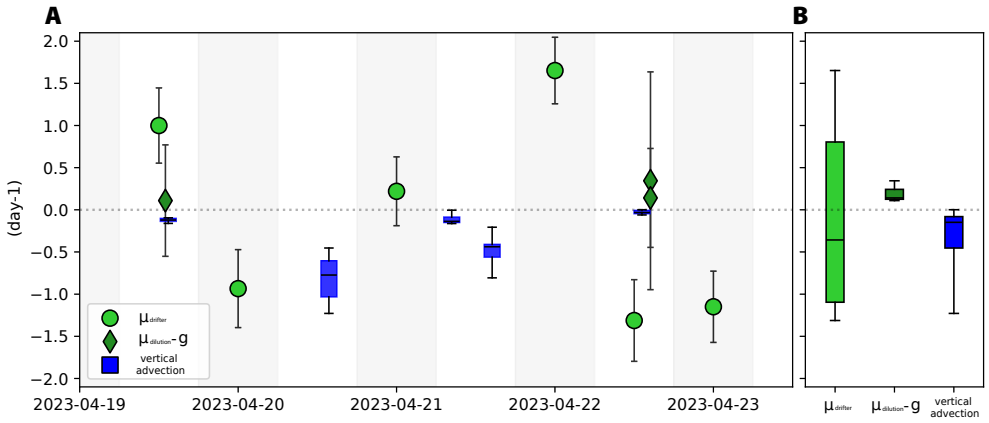

FIGURE 4. Relative contributions of physical vs biological processes. (a) Time-series of rates within 4 km of the eddy core for: specific chlorophyll growth rate μ_{drifter} averaged over 12-hours (nighttime vs daytime), net biological specific rate μ_{dilution} (growth minus grazing), and vertical advection contribution. Shaded areas represent nighttime (6pm-6am). (b) Total range of each budget term over the 4-day period, illustrating the relative contributions of biological to physical processes to chlorophyll variability.

surface divergence and is consistent with the typically short lifespan of submesoscale features that usually persist a few days to a couple of weeks.

Overall, the net contribution from biological processes to chlorophyll change is always positive, from 0.1 to 0.3 per day (Fig.4b). Sustained positive biological contributions require nutrient input, either through recycling or a non-linear response to upward advection. These processes can drive significant growth, thereby sustaining higher chlorophyll concentrations and potentially counteracting natural decay for a significant time period. Despite challenges in fully closing the chlorophyll variability budget due to data limitations, these estimates offer insights into the relative importance of each process in setting the surface chlorophyll within a submesoscale eddy, suggesting on the whole comparable contributions between biological and physical processes. This is in contrast to Lagrangian observations away from frontal zones, which found that grazing is the dominant process controlling distributions of phytoplankton carbon [37].

There are additional processes that should be considered to close the carbon budget. This analysis focuses on advective processes and we did not explicitly account for horizontal diffusion, or entrainment of surrounding waters during vertical advection, both of which could influence the contribution of physical processes [38]. Their contributions, although potentially small, remain an open question for future research and may be informative regarding the interaction of submesoscale eddies with background surface waters. In addition, it is important to note that while chlorophyll and biological rates represent integrated values over time (12 hours), vertical advection was calculated instantaneously due to data availability. The difference in temporal resolution may lead to an overestimation of the advective contributions to variability in our budget. Lastly, grazing was estimated from microzooplankton only, which are recognized as the dominant removal pathway for primary productivity globally [39]. Losses to mesozooplankton were not considered and may therefore lead to an overestimation of the biological contributions in our budget.

Discussion

This study shows that submesoscale eddies in the CCS can efficiently trap and transport nutrient-rich water offshore, contributing to POC enrichment in the otherwise nutrient-depleted region. The observed biophysical variability within the submesoscale feature arises from interactions across multiple dynamical scales. While upwelling and mesoscale eddies are generally viewed as the primary drivers of offshore productivity [5, 16, 3, 40, 31] and offshore organic matter transport in the CCS [41, 42], we find that coherent submesoscale eddies make a quantitatively important contribution to offshore carbon flux and highlight the interplay between biological and physical processes.

Submesoscale coherent eddies are commonly identified in satellite imagery as chlorophyll-rich features. However, due to the low resolution of satellite-derived velocity fields, it has not been previously possible to confirm whether these features are coherent submesoscale eddies, nor to quantify the relative contributions of vertical versus lateral nutrient transport. Here, we validate the coherence of one such feature and highlight the role of lateral trapping in the carbon content. Synthesizing these observations with the observational record from satellites, we estimate that submesoscale coherent eddies transport carbon cross-shore at a rate of -0.043 $\pm$ 0.024 mmol C m^{-2} s^{-1}. This is comparable to observed total organic carbon (TOC) mesoscale eddies cross-shore fluxes in a modeling study at up to –0.05 mmol C m^{-2} s^{-1} [6], as well as to other estimates of lateral nutrient fluxes across the gyre margin of the CCS [43, 8, 44]. These observations suggest that previous work may have underestimated the magnitude of carbon lateral flux from gyre margins to the open ocean, and raise uncertainty about the mechanisms.

Hotspots of biological productivity in the offshore region are known to be ecologically important [44] and the physical mechanisms governing their evolution and formation control their fate and productivity. Submesoscale coherent eddies, filaments, and mesoscale eddies represent dynamically distinct processes in this region. While an upscale energy cascade could cause submesoscale eddies to grow into mesoscale features, their formation mechanisms and early temporal evolution likely have important implications for biophysical processes, as we have detailed in this manuscript. These results suggest that trapping and lateral transport of POC-rich waters by submesoscale eddies are important mechanisms that contribute to maintaining biological productivity in the oligotrophic subtropical gyre. By contrast, if communities were not trapped in a coherent fashion, we anticipate that stirring into the background community would result in altered predator-prey dynamics and nutrient competition [45, 46, 47], with implications for plankton community structure [48, 49].

Submesoscale dynamics also significantly differ from mesoscale dynamics due to the amplified vertical motions associated with these features [50]. In this study, we observe evidence of vertical export of organic matter on the edges of the submesoscale eddy, which are consistent with other observations of subduction of filaments, including filaments with high biomass, around submesoscale or mesoscale eddy flow fields [51, 52, 53, 54]. This subduction alters the fate of surface nutrients and can lead to a leakage of organic nutrients from the upwelling zone.

Sparse data present a challenge for observational assessment of submesoscale dynamics and submesoscale biophysical coupling, often limiting the generalization of findings. To address this, this study tracks a submesoscale feature over an extended period of time, allowing for characterization of its spatial and temporal variability. Furthermore, we demonstrate how understanding of this feature facilitates extrapolation of regional scale implications.

Conclusion

Our results emphasize the role of submesoscale eddies in shaping offshore planktonic dynamics and eddy-driven carbon export in eastern boundary upwelling systems, by trapping and transporting coastal, nutrient-rich water in the oligotrophic subtropical gyre. Within submesoscale eddies, biophysical interactions bring large variability in surface chlorophyll concentrations. We suggest that, as it was demonstrated for mesoscale eddies [10, 6, 3], submesoscale eddies can be important to offshore transport of organic matter and create short-lived but dynamical ecological niches. While this study focuses on the CCS, these findings likely extend to other Eastern boundary currents given the ubiquitous presence of submesoscale eddies in the global ocean. Thus, their contribution to the global biological carbon pump needs to be considered. High-resolution measurements of both physical and biological processes in Eastern boundary currents are essential for improving our understanding of offshore marine ecosystems dynamics and the ocean carbon cycle.

Data availability All data needed to evaluate the conclusions in the paper are present in the paper and/or the Supplementary Materials. The code used for this analysis is available at `https://github.com/ebeaudin3/smode`.

Acknowledgments This work was supported by NASA grants 80NSSC24K1422, 80NSSC24M0143, and 80NSSC24K0410 to MAF. The authors thank Yue (Luna) Bai, Pierre Chabert, Lily Dove, Baylor Fox-Kemper, Shailja Gangrade, Kelly Luis, and Leo Middleton for insightful discussions. We are grateful to Kelly Luis and Roger Patrick Kelly for their assistance with data collection and calibration. We acknowledge the leadership of Chief Scientist Andrey Shcherbina and Principal Investigator J. Tom Farrar during the SMODE IOP2 campaign, and a special thanks to the captain and crew of the *R/V* Sally Ride.

References

[1] A Huyer, Coastal upwelling in the California current system. *Progress in Oceanography* **12**, 259–284 (1983).

[2] KH Brink, TJ Cowles, The Coastal Transition Zone program. *Journal of Geophysical Research: Oceans* **96**, 14637–14647 (1991).

[3] CM Amos, RM Castelao, PM Medeiros, Offshore transport of particulate organic carbon in the California Current System by mesoscale eddies. *Nature Communications* **10**, 4940 (2019).

[4] J Kurian, F Colas, X Capet, JC McWilliams, DB Chelton, Eddy properties in the California Current System. *Journal of Geophysical Research* **116**, C08027 (2011).

[5] N Gruber, et al., Eddy-induced reduction of biological production in eastern boundary upwelling systems. *Nature Geoscience* **4**, 787–792 (2011).

[6] T Nagai, et al., Dominant role of eddies and filaments in the offshore transport of carbon and nutrients in the California Current System. *Journal of Geophysical Research: Oceans* **120**, 5318–5341 (2015).

[7] SA Kranz, et al., Lagrangian Studies of Marine Production: A Multimethod Assessment of Productivity Relationships in the California Current Ecosystem Upwelling Region. *Journal of Geophysical Research: Oceans* **125**, e2019JC015984 (2020).

[8] M Gupta, et al., A nutrient relay sustains subtropical ocean productivity. *Proceedings of the National Academy of Sciences* **119**, e2206504119 (2022).

[9] K Oglethorpe, BF Castro, CP Spingys, AC Naveira Garabato, RG Williams, The Role of Mesoscale Eddy Stirring and Microscale Turbulence in Sustaining Biological Production in the Subtropical Gyres. *Global Biogeochemical Cycles* **39**, e2024GB008180 (2025).

[10] C Perruche, P Rivière, G Lapeyre, X Carton, P Pondaven, Effects of surface quasi-geostrophic turbulence on phytoplankton competition and coexistence. *Journal of Marine Research* **69**, 105–135 (2011).

[11] PT Strub, PM Kosro, A Huyer, The nature of the cold filaments in the California Current system. *Journal of Geophysical Research: Oceans* **96**, 14743–14768 (1991).

[12] X Álvarez Salgado, et al., Off-shelf fluxes of labile materials by an upwelling filament in the NW Iberian Upwelling System. *Progress in Oceanography* **51**, 321–337 (2001).

[13] F d'Ovidio, S De Monte, S Alvain, Y Dandonneau, M Lévy, Fluid dynamical niches of phytoplankton types. *Proceedings of the National Academy of Sciences* **107**, 18366–18370 (2010).

[14] SY Kim, Observations of submesoscale eddies using high-frequency radar-derived kinematic and dynamic quantities. *Continental Shelf Research* **30**, 1639–1655 (2010).

[15] M Lévy, PJS Franks, KS Smith, The role of submesoscale currents in structuring marine ecosystems. *Nature Communications* **9**, 4758 (2018).

[16] M Levy, AP Martin, The influence of mesoscale and submesoscale heterogeneity on ocean biogeochemical reactions. *Global Biogeochemical Cycles* **27**, 1139–1150 (2013).

[17] LN Thomas, A Tandon, A Mahadevan, Submesoscale processes and dynamics in *Geophysical Monograph Series*, eds. MW Hecht, H Hasumi. (American Geophysical Union, Washington, D. C.) Vol. 177, pp. 17–38 (2008).

[18] JC McWilliams, Submesoscale currents in the ocean. *Proceedings of the Royal Society A: Mathematical, Physical and Engineering Sciences* **472**, 20160117 (2016).

[19] TM Powell, et al., Spatial Scales of Current Speed and Phytoplankton Biomass Fluctuations in Lake Tahoe. *Science* **189**, 1088–1090 (1975).

[20] KL Denman, AE Gargett, Time and space scales of vertical mixing and advection of phytoplankton in the upper ocean. *Limnology and Oceanography* **28**, 801–815 (1983).

[21] A Mahadevan, The Impact of Submesoscale Physics on Primary Productivity of Plankton. *Annual Review of Marine Science* **8**, 161–184 (2016).

[22] F Chenillat, et al., Plankton dynamics in a cyclonic eddy in the Southern California Current System. *Journal of Geophysical Research: Oceans* **120**, 5566–5588 (2015).

[23] MA Freilich, G Flierl, A Mahadevan, Diversity of Growth Rates Maximizes Phytoplankton Productivity in an Eddying Ocean. *Geophysical Research Letters* **49**, e2021GL096180 (2022).

[24] L Seitz, M Freilich, Joint effects of submesoscale lateral dispersion and biological reactions on biogeochemical flux (2024).

[25] JT Farrar, et al., S-MODE: The Sub-Mesoscale Ocean Dynamics Experiment. *Bulletin of the American Meteorological Society* **106**, E657–E677 (2025).

[26] MR Landry, RP Hassett, Estimating the grazing impact of marine micro-zooplankton. *Marine Biology* **67**, 283–288 (1982).

[27] A Calbet, E Saiz, How much is enough for nutrients in microzooplankton dilution grazing experiments? *Journal of Plankton Research* **40**, 109–117 (2018).
[28] CS Roesler, AH Barnard, Optical proxy for phytoplankton biomass in the absence of photophysiology: Rethinking the absorption line height. *Methods in Oceanography* **7**, 79–94 (2013).
[29] S Lang, R Kelly, M Omand, S-MODE Bio-optical Data (V1) Report for IOP-2, Technical report (2023).
[30] TM Powell, et al., Results from a three-dimensional, nested biological-physical model of the California Current System and comparisons with statistics from satellite imagery. *Journal of Geophysical Research: Oceans* **111**, 2004JC002506 (2006).
[31] P Chabert, F d'Ovidio, V Echevin, MR Stukel, MD Ohman, Cross-Shore Flow and Implications for Carbon Export in the California Current Ecosystem: A Lagrangian Analysis. *Journal of Geophysical Research: Oceans* **126**, e2020JC016611 (2021).
[32] FJ Beron-Vera, Y Wang, MJ Olascoaga, GJ Goni, G Haller, Objective Detection of Oceanic Eddies and the Agulhas Leakage. *Journal of Physical Oceanography* **43**, 1426–1438 (2013).
[33] P Cetina-Heredia, M Roughan, E Van Sebille, S Keating, GB Brassington, Retention and Leakage of Water by Mesoscale Eddies in the East Australian Current System. *Journal of Geophysical Research: Oceans* **124**, 2485–2500 (2019).
[34] J Weiss, The dynamics of enstrophy transfer in two-dimensional hydrodynamics. *Physica D: Nonlinear Phenomena* **48**, 273–294 (1991).
[35] A Okubo, Horizontal dispersion of floatable particles in the vicinity of velocity singularities such as convergences. *Deep Sea Research and Oceanographic Abstracts* **17**, 445–454 (1970).
[36] JM D'Addezio, GA Jacobs, M Yaremchuk, I Souopgui, Submesoscale Eddy Vertical Covariances and Dynamical Constraints from High-Resolution Numerical Simulations. *Journal of Physical Oceanography* **50**, 1087–1115 (2020).
[37] MR Landry, MD Ohman, R Goericke, MR Stukel, K Tsyrklevich, Lagrangian studies of phytoplankton growth and grazing relationships in a coastal upwelling ecosystem off Southern California. *Progress in Oceanography* **83**, 208–216 (2009).
[38] D Li, X Ruan, A Le-Duy Pham, P Damien, D Bianchi, Role of Eddies in Primary Production in the California Current System. *Geophysical Research Letters* **52**, e2025GL118614 (2025).
[39] A Calbet, MR Landry, Phytoplankton growth, microzooplankton grazing, and carbon cycling in marine systems. *Limnology and Oceanography* **49**, 51–57 (2004).
[40] TTM Hong, YG Park, JM Choi, Divergence Observation in a Mesoscale Eddy during Chla Bloom Revealed in Submesoscale Satellite Currents. *Remote Sensing* **15**, 995 (2023).
[41] X Capet, JC McWilliams, MJ Molemaker, AF Shchepetkin, Mesoscale to Submesoscale Transition in the California Current System. Part I: Flow Structure, Eddy Flux, and Observational Tests. *Journal of Physical Oceanography* **38**, 29–43 (2008).
[42] DP Dauhajre, JC McWilliams, Y Uchiyama, Submesoscale Coherent Structures on the Continental Shelf. *Journal of Physical Oceanography* **47**, 2949–2976 (2017).
[43] RT Letscher, F Primeau, JK Moore, Nutrient budgets in the subtropical ocean gyres dominated by lateral transport. *Nature Geoscience* **9**, 815–819 (2016).
[44] M Messié, DA Sancho-Gallegos, J Fiechter, JA Santora, FP Chavez, Satellite-Based Lagrangian Model Reveals How Upwelling and Oceanic Circulation Shape Krill Hotspots in the California Current System. *Frontiers in Marine Science* **9**, 835813 (2022).
[45] AP Martin, KJ Richards, A Bracco, A Provenzale, Patchy productivity in the open ocean. *Global Biogeochemical Cycles* **16** (2002).
[46] Y Lehahn, F d'Ovidio, M Lévy, E Heifetz, Stirring of the northeast Atlantic spring bloom: A Lagrangian analysis based on multisatellite data. *Journal of Geophysical Research: Oceans* **112**, 2006JC003927 (2007).
[47] Z Neufeld, Stirring effects in models of oceanic plankton populations. *Chaos: An Interdisciplinary Journal of Nonlinear Science* **22**, 037102 (2012).
[48] F d'Ovidio, S De Monte, S Alvain, Y Dandonneau, M Lévy, Fluid dynamical niches of phytoplankton types. *Proceedings of the National Academy of Sciences* **107**, 18366–18370 (2010).
[49] R Tzortzis, et al., The contrasted phytoplankton dynamics across a frontal system in the southwestern Mediterranean Sea. *Biogeosciences* **20**, 3491–3508 (2023).
[50] JR Taylor, AF Thompson, Submesoscale Dynamics in the Upper Ocean. *Annual Review of Fluid Mechanics* **55**, 103–127 (2023).
[51] MM Omand, et al., Eddy-driven subduction exports particulate organic carbon from the spring bloom. *Science* **348**, 222–225 (2015).

[52] M Archer, et al., Observations of Submesoscale Variability and Frontal Subduction within the Mesoscale Eddy Field of the Tasman Sea. *Journal of Physical Oceanography* **50**, 1509–1529 (2020).
[53] MA Freilich, et al., 3D intrusions transport active surface microbial assemblages to the dark ocean. *Proceedings of the National Academy of Sciences* **121**, e2319937121 (2024).
[54] H Cao, et al., Isopycnal Submesoscale Stirring Crucially Sustaining Subsurface Chlorophyll Maximum in Ocean Cyclonic Eddies. *Geophysical Research Letters* **51**, e2023GL105793 (2024) _eprint: https://agupubs.onlinelibrary.wiley.com/doi/pdf/10.1029/2023GL105793.

[a] Department of Earth, Environmental & Physical Sciences, Brown University, Providence, RI, 02912, USA

[b] Integrative Oceanography Division, Scripps Institution of Oceanography, University of California San Diego, La Jolla, CA, 92037, USA

[c] Graduate School of Oceanography, University of Rhode Island, Narragansett, RI, 02882, USA

[d] Division of Applied Mathematics, Brown University, Providence, RI, 02912, USA